Catalysis Today 418 (2023) 114039

Contents lists available at ScienceDirect

Catalysis Today

journal homepage: www.elsevier.com/locate/cattod

Carbon dots as green photocatalysts for atom transfer radical polymerization of methacrylates

Carlotta Campalani, Nicola Bragato, Andrea Morandini, Maurizio Selva, Giulia Fiorani *, Alvise Perosa *

Department of Molecular Sciences and Nanosystems, Università Ca' Foscari di Venezia, Via Torino 155, 30172 Venezia, Mestre, Italy

ARTICLE INFO

Keywords:
Photocatalysis
Carbon dots
Atom transfer radical polymerization
Methacrylates

ABSTRACT

We herein report the use of carbon dots (CDs) in photoinduced atom transfer radical polymerizations (ATRP) as green metal-free sensitizers. In particular, the production of a polymethacrylate (poly-METAC, METAC = 2-(methacryloyloxy)ethyl]trimethylammonium chloride) by using cheap and easily affordable CDs made from citric acid and diethylenetriamine, under both ultraviolet (UV, λ = 365 nm) and visible light was studied. Different solvent systems have been tested and a Cu^{II} complex was used as catalyst. Under the best conditions a polymer in 89% conversion and with a narrow dispersity (1.4) was obtained. The first order kinetics and the "on-off" experiments gave further evidence of the constant concentration of radicals and of the controlled mechanism of the polymerization.

1. Introduction

Since 1995, when atom transfer radical polymerizations (ATRP) were reported for the first time, immense progresses have been developed in the field of synthetic polymers [1–3]. Indeed, differently from ionic or radical polymerizations, ATRP processes are not too sensitive to the reaction conditions, can be initiated by different active and versatile metal-based catalytic systems, leading to well-defined polymers and controlled architectures, and can be applied to a plethora of different monomers [4]. ATRP are redox processes mediated by the reversible reaction between a low oxidation state complex as catalyst, commonly Cu^{II} complexes although other transition metals have also been used, and an alkyl halide acting as initiator [5]. This activation process implies oxidation of the metal catalyst ($Mt^n \rightarrow Mt^{n+1}$) with formation of an active specie that initiates the polymerization. The subsequent deactivation pathway comprises addition of the monomer with formation of the initial dormant species and reduction of the catalyst to its former low oxidation state. One of the major drawbacks of ATRP is the necessity to use large amounts of catalyst in order to have better control over the whole polymerization process. Lately, to overcome environmental and practical issues, different initiation techniques to generate in situ the metal catalyst have been reported. These methods focus on different reduction pathways for the formation of the activator Mt^n species, and, to date, they have been conducted using different reducing agents [6], electrochemical processes [7], copper-containing nanoparticles,[8] and photochemical redox processes [9–14]. Referring to the latter protocol, it must be noticed how light is an environmental friendly, widely available and non-invasive reagent that can lead to spatial and temporal control of different ATRP processes [15]. Scheme 1 reports the common pathway for photoinitiated ATRP where the photosensitizer manages to reduce a metal complex (X-Mt^{n+1}/L) to the correspondent active catalyst (Mt^n/L). The catalyst, then, proceeds with the formation of the active specie from the initiator (P_n-X → P_n·) that starts the polymerization of the monomer (M), with consequent re-oxidation of the metal complex (X-Mt^{n+1}/L).

Different photoactive molecules (e.g. dyes or commercial photoinitiators) proved to be effectives reducing agents facilitating the photoinitiated ATRP process. Therefore, in situ photolytic generation of the reduced complex under irradiation enables polymerization also with small concentrations of catalyst [16]. In addition, the polymerization reaction can be stopped and restarted easily by switching on and off the light source. Photoinduced ATRP has been successfully performed using different sources of light, from UV [10,12,] to visible [17], or near infrared [18]. Nevertheless, there are still some drawbacks and challenges to overcome. In particular, the majority of the photosensitizers tested for photo-ATRP relies on synthetic pathways that are not sustainable and can be harmful for the environment and the user. In this framework, carbon dots (CDs) based on natural feedstocks represent

* Corresponding authors.
E-mail addresses: giulia.fiorani@unive.it (G. Fiorani), alvise@unive.it (A. Perosa).

https://doi.org/10.1016/j.cattod.2023.114039
Received 1 December 2022; Received in revised form 8 February 2023; Accepted 10 February 2023
Available online 12 February 2023

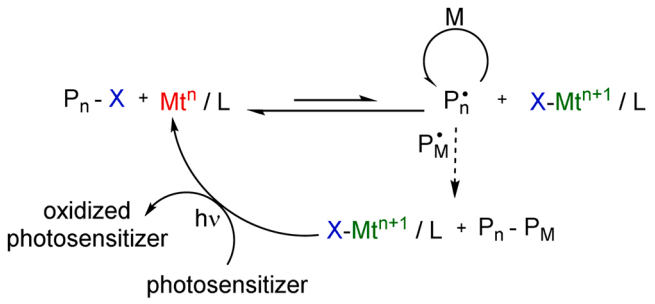

Scheme 1. General mechanism of the equilibrium in ATRP processes with regeneration of the activator via electron transfer induced by light. Mt^n/L is the metal catalyst, P_n-X the initiator, M the monomer and P_M the growing polymer chain.

emerging, environmentally friendly alternatives. The first example regarding the use of these nanoparticles in a photo-controlled radical polymerization was reported only recently, employing phosphorus and sulfur-doped CDs deriving from ascorbic acid for photoinduced reversible addition-fragmentation chain-transfer polymerization [19]. In addition, in 2020, CDs produced from sodium alginate and ethylenediamine were employed for the first time for photo-ATRP of methylmethacrylate in dimethylsulfoxide, yielding polymers with a narrow dispersity and low (30%) conversion [16]. Under irradiation, indeed, CDs can be excited and act as reducing agents to obtain Cu^I from Cu^{II} in the polymerization system: the thus formed Cu^I complex reacts with a bromine initiator and forms active free radicals that initiate the polymerization.

CDs are carbon nanoparticles with a quasi-spherical shape and dimensions below 10 nm that have shown excellent photoactivity. These nanoparticles are mainly composed by a carbogenic core (amorphous or graphitic) and a highly functionalized surface with organic functional groups, molecular fluorophores and defects. The promising properties of CDs, such as biocompatibility, non-toxicity, electron donor/acceptor ability, water solubility and ease in preparation and functionalization, led to a wide range of different applications. Among them, CDs have been already used for bioimaging [20], drug delivery, [21] as well as optoelectronic and energy-related applications [22,30]. In addition, CDs have been employed in photocatalytic applications,[23–25] displaying activity towards photooxidations, photodegradations and photoreductions [26–29]. CDs can be easily synthetized from cheap and abundant carbon precursors and their preparation is easily tailored by the choice of the synthetic method (i.e. hydrothermal treatment, pyrolysis, microwave and so on) and by the addition of doping agents that can enhance their photoactivity [24,25]. Doping, in fact, has been demonstrated to be an effective method to customize the optical, electrical and chemical properties of CDs, resulting in a variety of different CDs for specific requirements [31–33]. One of the most used doping agent is nitrogen that is known to increase the quantum yield (number of emitted photons on number of absorbed photons %) of the CDs, an important parameter in the preparation of effective photocatalysts [34].

In this contribution we studied the possibility of developing CDs photosensitizers derived from citric acid and diethylenetriamine for an efficient photoinduced ATRP of a methacrylate (METAC = 2-(methacryloyloxy)ethyl]trimethylammonium chloride) by irradiating both under UV ($\lambda = 365$ nm) and visible light. Compared to the existing literature, the polymerization performed in the present investigation focused on using greener water-based solvents and managed to reach higher monomer conversions (up to 89%) with a narrow dispersity [16].

2. Experimental section

2.1. Materials and methods

All the reagents were purchased from Merck Life Science S.r.l. (Milano, Italy), were of analytical grade and used without further purification. MilliQ water, used as a solvent throughout the experiment, was obtained with a Merck Millipore C79625 system.

CHNS analysis was performed with an Elemental Unicube instrument. Optical characterization of CDs was performed with an Agilent 8456 UV–Vis spectrophotometer. ^{1}H and ^{13}C{^{1}H} NMR spectra were recorded on a Bruker AV 400 (^{1}H: 400 MHz; ^{13}C: 100 MHz) spectrometer. The chemical shifts (δ) were reported in parts per million (ppm) relative to the residual undeuterated solvent signal as internal reference. Gel permeation chromatography (GPC) was performed on an Agilent Infinity 1260 system equipped with refractive index detector, using an injection volume of 20 μL and a flow rate of 1 mL/min. A Phenomenex PolySep linear was used as column maintaining a constant temperature of 40 °C during the analysis. An aqueous solution of LiCl 0.1 M was used as eluent and polyethylene glycol was used as standard. DSC analyses were performed on a Mettler Toledo DSC 3 analyser under air atmosphere. The temperature of the instrument was calibrated using indium as standard. Poly-METAC (about 10.0 mg) was weighed into aluminium oxidized melting pots, sealed, and heated from room temperature to 300 °C at 10 °C/min. An empty sealed melting pot was used as reference. Thermogravimetric analyses were performed using a Perkin Elmer TGA 4000 instrument. The analyses were carried out weighting 10.0 mg of poly-METAC in a ceramic crucible, in a temperature range from 30 °C to 600 °C with a heating rate of 10 °C/min and under a nitrogen flow of 20 mL/min.

2.2. Synthesis of cit-CDs

The non-doped nanoparticles were hydrothermally synthesized as already reported [24]. In detail, 2 g of citric acid were dissolved in 20 mL of MilliQ; the solution was heated in a sealed stainless steel autoclave for t = 24 h at T = 180 °C. The mixture was then neutralized to neutral pH with an aqueous NaOH solution, filtered on paper (porosity 8–12 μM) and evaporated to dryness leading to a dark yellow luminescent oil (25% wt. yield) which was used without any further purifications. The obtained nanoparticles have been characterized via NMR, UV-Vis and CHNS elemental analysis.

2.3. Synthesis of N-cit-CDs

The nitrogen doped CDs were hydrothermally synthesized by heating an aqueous solution of citric acid (2 g in 20 mL of MilliQ water) and diethylenetriamine (0.67 g) in a sealed autoclave for t = 6 h at T = 180 °C [25]. The mixture was then filtered (porosity 8–12 μM) and evaporated to dryness leading to a brown solid (72% wt yield) which was used without any further purifications. The obtained nanoparticles have been characterized via NMR, UV-Vis and CHNS elemental analysis.

2.4. Synthesis of 2-hydroxyethyl-2-brom-2-methylpropanoate (HEBIB)

For the synthesis of the initiator, 1.5 mol of ethylene glycol and 60 mmol of triethylamine were dissolved in 30 mL of anhydrous tetrahydrofuran and placed in a round bottom flask. The reaction flask was put under inert atmosphere and kept under stirring in an ice bath while adding dropwise (in 30 min) 30 mmol of α-bromoisobutyryl bromide. After stirring at room temperature for t = 16 h, 200 mL of deionized water were added to the flask and the product was extracted with dichloromethane (3 ×30 mL). The organic fraction was washed with 30 mL of an aqueous solution of HCl (1 M). The solvent was removed in vacuo leading to HEBIB as a yellow oil in 94.5% yield. ^{1}H NMR (400 MHz, $CDCl_3$, 298 K) δ: 1.96(s, 6 H), 3.87 (t, 2 H), 4.31 (t, 2 H). ^{13}C

NMR (100 MHz, $CDCl_3$, 298 K) δ: 30.7, 55.8, 60.7, 63.3, 67.4, 171.8.

2.5. ATRP experiments with CDs

10 mmol of [2-(methacryloyloxy)ethyl]trimethylammonium-chloride (METAC), 0.1 mmol of 2-hydroxyethyl-2-brom-2-methylpropanoate (HEBIB), 6.3 mg of CDs (N-cit-CDs or Cit-CDs) and 1 mL of an aqueous solution of $CuBr_2$ and N,N′,N″,N″ pentamethyldiethylenetriamine ($CuBr_2$ (0.1 mmol), PMDTA (0.3 mmol), were added to a Schlenk tube. The chosen solvent was added in quantity equal to the volume of monomer and $CuBr_2$/PMDTA solution. After 5 vacuum/nitrogen cycles the reactor was kept under continuous stirring and irradiation (LEDs; UV, fixed wavelength $\lambda = 365$ nm, Hangar s.r.l.; ATON LED-UV 365; 80 W/m^2 of irradiance in the UVA spectral range 315–400 cm^{-1}, or Vis = 5400 K, 16 W, 12 V, 1.5 A) for t = 1 h. The sample was placed at a distance of 10 cm from the LEDs light source.

The polymer product was precipitated using acetone as counter solvent. After solvent removal, the product was dissolved in methanol concentrated by rotary evaporation and dried in vacuo at T = 70 °C (p = 80 mbar) overnight. The product was obtained as a glassy, transparent solid and characterized via NMR, DSC and TGA.

2.6. ATRP experiments without CDs

10 mmol of [2-(methacryloyloxy)ethyl]trimethylammonium-chloride (METAC), 0.1 mmol of 2-hydroxyethyl-2-brom-2-methylpropanoate (HEBIB) and 0.25 mmol of N,N′,N″,N″ pentamethyldiethylenetriamine (PMDTA), were added to a Schlenk tube. The chosen solvent (1:1 mixture water:methanol) was added in quantity equal to the volume of monomer. After 3 vacuum/nitrogen cycles, 0.1 mmol of CuBr were added in the reactor under abundant nitrogen flow to preserve the inert atmosphere. After additional 3 vacuum/nitrogen cycles, the system was kept under continuous stirring for 12 h. The polymer product was precipitated using acetone as counter solvent. After remotion of the solvent, the product was dissolved in methanol subsequently removed by rotary evaporation. The polymer was kept in vacuum oven at T = 70 °C (p = 80 mbar) overnight.

3. Results and discussion

3.1. CDs synthesis and characterization

As novel type of photosensitizer to activate the ATRP, two different types of CDs has been tested. Using always citric acid as the carbon source, doped (N-cit-CDs) and non-doped (cit-CDs) nanoparticles were obtained through a bottom-up synthetic technique (see Section 2.2. and 2.3.). These two families of CDs have already been synthesized and tested for their photocatalytic performances elsewhere [24,27,35]. In our previous studies, extensive HR-TEM, FT-IR, UV-Vis, XPS, PL/PLE, ESI-MS, ^1H/ $^{13}C\{^1H\}$ NMR and DOSY analyses indicated the amorphous nature of both nanoparticles. Concerning cit-CDs, from HR-TEM it was possible to observe nanoparticles with a poorly defined shape and diameters ranging from 9 to 12 nm [24], while for N-cit-CDs diameters in the range of 13 nm were confirmed via atomic force microscopy [27]. FT-IR of cit-CDs showed strong broad adsorptions in the region 3500–3000 cm^{-1} related to the O-H stretching, weak signals for the C-H stretching at 2900–2800 cm^{-1}, peaks at 1722 or 1738 cm^{-1} assigned to the C═O stretching of carboxylic acids and signals at 1626 or 1633 cm^{-1} due to aromatic C═C stretching. Concerning the N-cit-CDs, the same peaks were observed together with new peaks due to the presence of nitrogen. In particular, a signal around 3300–3000 cm^{-1} highlighted the N-H stretching and another one around 3000–2800 was reasonably assigned to the presence of ammonium groups. XPS analysis of the cit-CDs showed C and O in the ratios 45/55 and confirmed the presence of C═C, C − O, and C═O functional groups. In the case of N-cit-CDs, the high-resolution XPS spectra highlighted a C, O, and N ratio of 70/20/10 and confirmed again the FT-IR assignments, and the N 1 s peak shows two bands related to both pyridinic environments or $-NH_2$ groups and to the C−N − C groups [35]. As can be seen in Fig. 1, both CDs are able to absorb in the UV region (350 nm n- π* transition and 250 nm π -π*), but in the case of N-cit-CDs, it was possible to observe a more evident absorption also in the visible range: this evidence prompted us to test this class of nanoparticles also for visible light photoinduced ATRP. In addition, the ability of nitrogen doping for the enhancement of the activation of this type of polymerizations has been demonstrated: in the *N*-doped electron-rich carbon nanostructure, the π electrons were activated by its conjugation with the lone pair electron of nitrogen, resulting in excellent electrochemical and catalytic performances [32,36]. The amount of nitrogen doping in N-Cit-CDs was evaluated via elemental analysis showing a carbon/nitrogen ratio equal to 3.2.

3.2. ATRP experiments

The ability of CDs to mediate photoinduced ATRP was tested irradiating (UV light $\lambda = 365$ nm LEDs and visible light 5600 K LEDs) solutions of CDs in different solvent systems (water, water/methanol and water/acetonitrile) with 2-hydroxyethyl-2-brom-2-methylpropanoate (HEBIB, see synthetic procedure in Section 2.4.) as the initiator together with the $CuBr_2$/ *N*,*N*,*N*′,*N*″,*N*″-pentamethyldiethylenetriamine (PMDTA) complex as the catalyst for the polymerization of [2-(methacryloyloxy)ethyl]trimethylammonium chloride (METAC)] under inert atmosphere (N_2). A proposed mechanism on the role of CDs is reported in Scheme 2. After irradiation, the photoexcitation of CDs results in the population of the excited state (CDs*) that can perform an electron transfer to $[Cu^{II}$ PMDTA$]Br_2$. This results in the reduction of the Cu^{II} complex to the respective Cu^{I} form that can initiate the radical polymerization of the alkyl bromide (HEBIB). The feasibility of CDs to reduce the Cu^{II} complex is supported also by the analysis of the redox potentials of the species. As reported in our previous study, N-cit-CDs possess $E_{red} = -1.94$ V and $E_{ox} = +1.12$ V, and cit-CDs $E_{red} = -1.83$ V and $E_{ox} = +0.52$ V,[25] while the redox potentials of the Cu complex are reported to be $E_{red} = -0.155$ V and $E_{ox} = -0.045$ V[37]. These data prompted us to test both the synthesized CDs for the activation of the metal catalyst.

The regeneration of CDs takes place in the photocatalytic cycle, when the oxidized CDs (CDs $^{\bullet+}$) react with bromide [16]. Scheme 2 reports different possible polymer termination pathways such as radical disproportionation, combination of two active chain ends or halogen termination. In the latter case, the polymer itself can become new initiator restarting the cycle. All the experiments were conducted at room temperature, under different light sources and in different solvents, with constant ratio between the reagents [METAC]/[HEBIB]/[CDs]/[$CuBr_2$]/[PMDTA] = 100:1:1:1:3 mol/mol and constant exposure time (1 h). Lower ratios of catalyst ([METAC]/[$CuBr_2$]/[PMDTA] = 100:0.1:0.3, 100:0.25:0.75 and 100:0.5:1.5 mol/mol) have also been tested but no production of polymer was observed (see Table S2 in the Supporting Information).

3.2.1. ATRP of METAC under UV irradiation

The investigation started by testing the photoinitiation activity of CDs under UV irradiation at $\lambda = 365$ nm. Three different solvent system were tested, namely water, water/methanol and water/acetonitrile. As can be seen in Table 1, using the doped CDs (entries 1, 2 and 3) high conversions of the monomer (from 85% to 89%) were obtained in all the three solvents after only 1 h of light exposure. The obtained polymers showed dispersity (Đ) always < 2 demonstrating a good control over the polymerization reaction. Nevertheless, changing the solvents, some differences concerning the weight-average molar mass, number-average molar mass and dispersity were observed. The 1:1 mixture of water and methanol was selected as the best performing environment resulting in slightly higher conversions (89%, entry 2, Table 1) and narrower

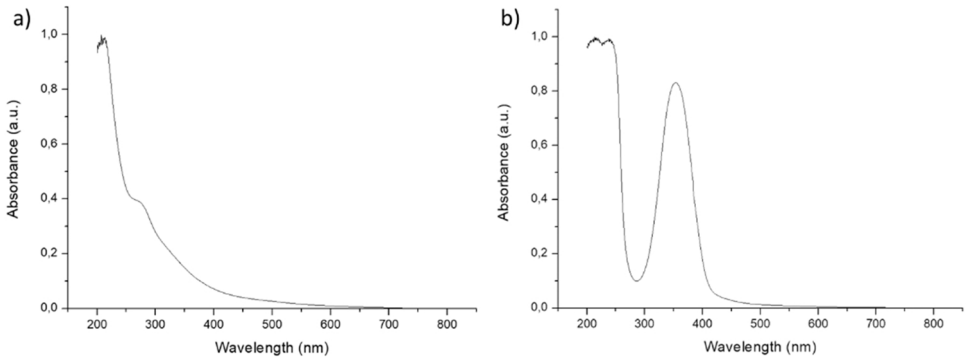

Fig. 1. UV-Vis spectra of the synthesized CDs. a) non doped cit-CDs; b) doped N-Cit-CDs.

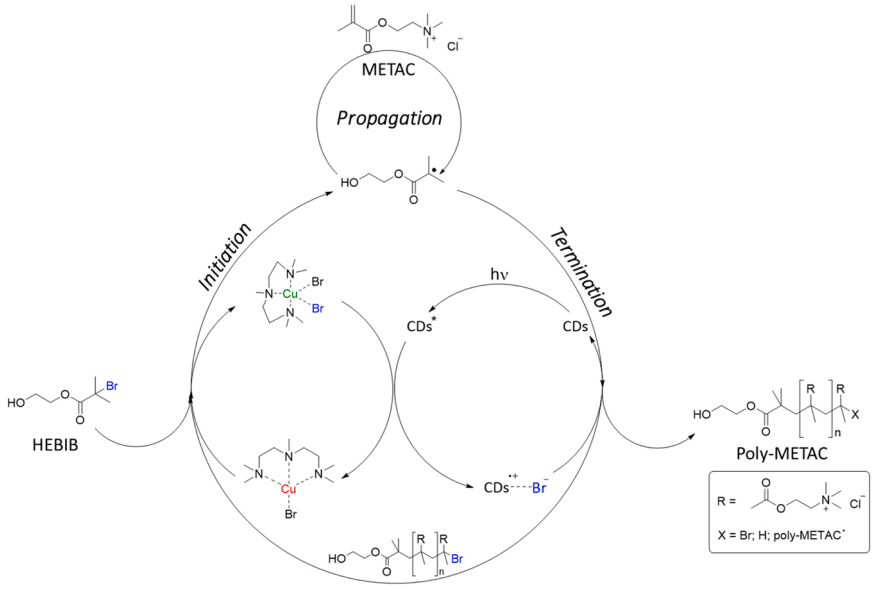

Scheme 2. Proposed mechanism for photoinduced ATRP of METAC using CDs.

Table 1
UV light (λ = 365 nm) induced ATRP of METAC using different CDs and in different solvents. [a].

Entry	CDs	Solvent	Conversion (%)[b]	M_n ($g \cdot mol^{-1}$)[c]	M_w ($g \cdot mol^{-1}$)[c]	Đ[c]
1	N-cit-CDs	Water	88	1600	2500	1.5
2	N-cit-CDs	H_2O/MeOH 1:1 V/V	89	1896	2655	1.4
3	N-cit-CDs	H_2O/CH_3CN 1:1 V/V	85	1430	2610	1.8
4	Cit-CDs	H_2O/MeOH 1:1 V/V	n.d.[d]	n.d.[d]	n.d.[d]	n.d.[d]
5	-	H_2O/MeOH 1:1 V/V	n.d.[d]	n.d.[d]	n.d.[d]	n.d.[d]

[a] Experiments were conducted at r.t. for t = 1 h using a ratio [METAC]/[HEBIB]/[CDs]/[$CuBr_2$]/[PMDTA] = 100:1:1:1:3 mol/mol; [b] determined gravimetrically; [c] determined by gel permeation chromatography using PEG standards; [d] confirmed via GPC: only molecular weights < 200 $g \cdot mol^{-1}$ were observed.

dispersity (1.4).

To gain further insight into the mechanism of polymerization, an experiment using the same conditions but in absence of CDs was performed (Table 1, entry 5). In this case no polymer was obtained demonstrating the necessity to photoactivate the copper catalyst. Other blank tests, namely in absence of light, catalyst and without CDs/irradiation, were performed to confirm the importance of all the components for photoinduced ATRP of METAC. All the blank tests were performed using the 1:1 mixture of water and methanol as the designed solvent and in all tested condition no formation of polymer was observed (see Table S1 in the Supporting Information).

Once selected the optimized reaction conditions, a kinetic study was performed to confirm the linear increase of the conversion during the irradiation time. As shown in Fig. 2, a linear correlation between the logarithm of monomer concentration (ln $[M_0]/[M_t]$) and time (t, starting at t = 0), highlighted a first order kinetic. This evidence indicates that the concentration of active free radicals can be seen as constant during the reaction [16,38].

To better understand the influence of the nitrogen doping in the photosensitizer, non-doped CDs (Cit-CDs) were tested in the best conditions found for N-cit-CDs (Table 1, entry 4). However, the non-doped nanoparticles did not show a consistent activity in activating the copper catalyst and no polymer was detected after 1 h of irradiation. This result strengthens the importance of nitrogen doping in CDs in order to obtain valuable photosensitizers.

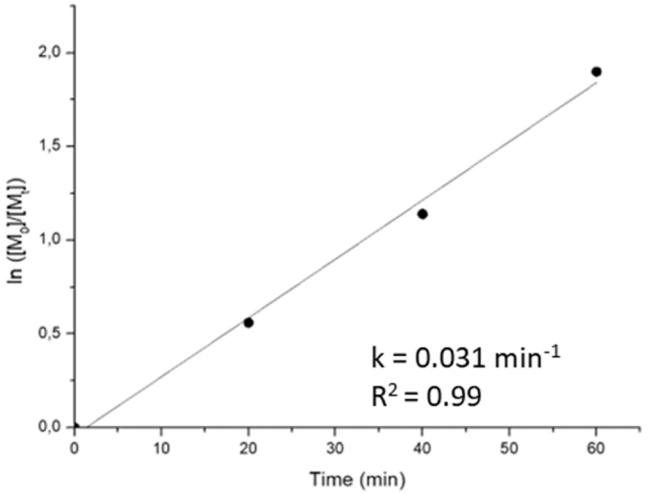

Fig. 2. Kinetic plot of the polymerization system using N-cit-CDs under UV irradiation and relative rate constant. Conditions reported in Table 1, entry 2.

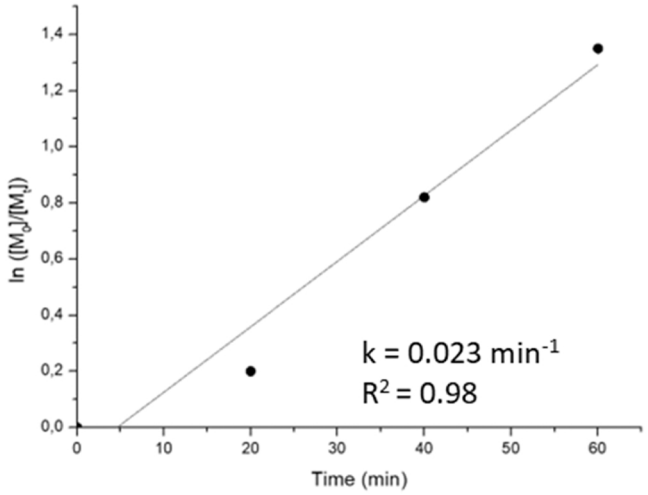

Fig. 3. Kinetic plot of the polymerization system using N-cit-CDs Under Vis irradiation and relative rate constant. Conditions reported in Table 2, entry 2.

3.2.2. *ATRP of METAC under visible light irradiation*

Concerning visible light, the non-doped CDs were not used since they have negligible absorbance in the visible region (see UV spectrum in Fig. 1). As for UV exposed experiments, three different solvents were examined but, in this case only using water/methanol 1:1 V/V it was possible to observe the presence of the polymer (Table 2, entry 2). After 1 h of irradiation, poly-METAC was obtained with 70% conversion and a narrow dispersity (1.5) highlighting the possibility to activate this reaction using visible light as a green, cheap and safe reagent.

An experiment under the same conditions but without the addition of CDs has been performed (Table 2, entry 4) but no polymer was detected, underlying once again the pivotal role of CDs in the activation step. Another blank test in absence of the copper catalyst was performed and, also in this case, no poly-METAC was observed (see Table S1 in the Supporting Information).

To further confirm the linear correlation between monomer concentration and irradiation time, a kinetic study was conducted also under Vis light. As can be seen in Fig. 3, a first order kinetic was observed indicating once again an almost constant concentration of free radicals during the polymerization. The difference in the rate constant of the ATRP under UV irradiation ($k = 0.031\ min^{-1}$) and visible one ($k = 0.023\ min^{-1}$) underlined the higher speed of the polymerization at 365 nm, confirming a major activity of the carbon nanoparticles at that wavelength.

Table 2
Visible light (5600 K) induced ATRP of METAC using N-cit-CDs in different solvents.[a].

Entry	CDs	Solvent	Conversion (%)[b]	M_n ($g \cdot mol^{-1}$)[c]	M_w ($g \cdot mol^{-1}$)[c]	Đ[c]
1	N-cit-CDs	Water	n.d.[d]	n.d.[d]	n.d.[d]	n.d.[d]
2	N-cit-CDs	H_2O/MeOH 1:1 V/V	70	1460	2170	1.5
3	N-cit-CDs	H_2O/CH_3CN 1:1 V/V	n.d.[d]	n.d.[d]	n.d.[d]	n.d.[d]
4	-	H_2O/MeOH 1:1 V/V	n.d.[d]	n.d.[d]	n.d.[d]	n.d.[d]

[a] Experiments were conducted at r.t. for t = 1 h using a ratio [METAC]/[HEBIB]/[CDs]/[$CuBr_2$]/[PMDTA] = 100:1:1:1:3 mol/mol; [b] determined gravimetrically; [c] determined by gel permeation chromatography using PEG standards; [d] confirmed via GPC: only molecular weights < 200 $g \cdot mol^{-1}$ were observed.

3.3. *Polymer characterization*

The characterization of the obtained polymer has been conducted using gel permeation chromatography (Tables 1 and 2), thermogravimetric analysis, differential scanning calorimetry and NMR (spectra in Figs. S1 and S2, Supporting Information). The product resulted as a thermoplastic, amorphous and transparent polymer with a glass transition temperature (T_g) of 100 °C (see Fig. S3, Supporting Information), similar to polymethylmethacrylate (T_g = 110 °C). The thermogravimetric analysis of the polymer (Fig. S4, Supporting Information) showed a first small weight loss (ca. 2.5 wt%) at T = 100 °C due to the dehydration of water in the polymer and elimination of residual humidity [39]. The second stage, between 280 and 300 °C, corresponds to the thermal decomposition of the groups that protruded from the polymer chain [40], while, the third weight loss at 390–400 °C, is ascribed to exothermic decomposition of the ammonium salts.[41] The obtained poly-METAC retained the luminescence properties of the CDs revealing the presence of part of the photo-initiator trapped in the polymeric mass (see Fig. S5, Supporting Information). In order to understand if the presence of the CDs affects the characteristics of the polymer, a classical ATRP of METAC has been conducted (see experimental Section 2.6) and the obtained material was characterized and compared with the poly-METAC obtained with CDs. The two polymers had the same aspect and consistency being transparent and amorphous and no substantial differences were highlighted from TGA and DSC analyses (Figs. S6 and S7, Supporting Information). The only difference is luminescence. For these reasons, the presence of CDs in the polymer matrix was not considered detrimental but it only add luminescence properties to the material that can be interesting for special applications.

3.4. *"On-off" experiment*

Light "on-off" experiments were performed both under UV (conditions in Table 1, entry 2) and Vis light (conditions in Table 2, entry 2). The polymerization mixtures were subjected to repeated light exposure by irradiating the sample for 20 min and then kept in dark for 10 min. The obtained results (Fig. 4) highlighted the dependence of the polymerization on the irradiation: no polymerization occurred when the solutions were kept in a dark environment. During the light exposure time, light induced ATRP were carried out showing also the different polymerization rates under UV and visible light. However, we expected the CDs to simply initiate the process that then should proceed without

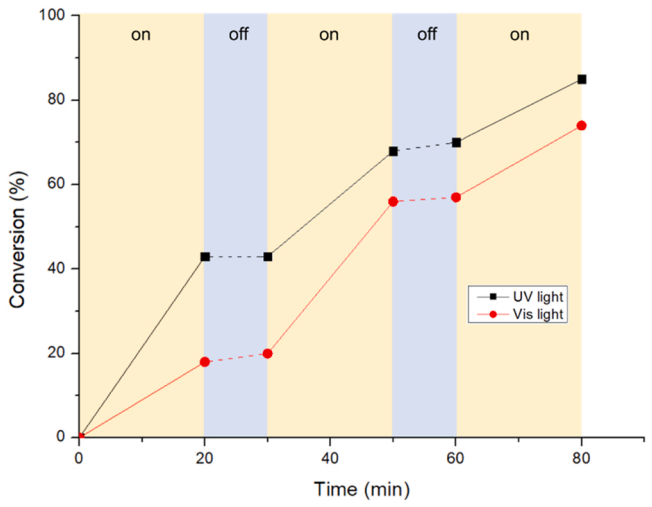

Fig. 4. Monomer conversion (%) versus time using CDs to determine the dependency on irradiation (UV = black line, Vis = red line). Yellow regions refer to light on, blue regions to light off. The UV irradiated experiment was performed following the conditions reported in Table 1, entry 2; the Vis irradiated following the conditions in Table 2, entry 2.

further photochemical input. This apparent contradiction can be explained by the fact that typical lifetimes for radical chain processes happens on the timescale of seconds or sub-seconds: conversions that terminate during the dark periods could relate to chain processes that terminate faster than the timescale of the analytical measurement. The observation that poly-METAC is formed only upon constant irradiation suggests that the photocatalytic reaction might be susceptible to temporal and spatial control. This behaviour, however, can evidently still manifest in photocatalytic transformations involving long chain reactions, highlighting the urge in being cautious in drawing conclusions about chain propagation from "*on-off*" experiments [42].

4. Conclusions

We report an efficient photoinduced atom transfer radical polymerization (ATRP) protocol activated by citric acid-derived CDs. In particular, nitrogen doped carbon nanoparticles were synthesized and used as photosensitizer for the preparation of poly-METAC (2-(methacryloyloxy)ethyl]trimethylammonium chloride) with a greener and sustainable synthetic procedure. The reaction, indeed, was found to be efficient in water-based solvent, in particular in water/methanol (1:1) solution, and the presence of a photosensitizer allowed to use small amounts of metal catalyst (1% mol based on the monomer). It should be highlighted that N-cit-CDs are able to activate the polymerization under both UV and visible light, paving the way towards an eco-friendly, cheap and affordable synthetic procedure for the obtainment of polymethacrylates. After only 1 h of irradiation it was possible to retrieve the polymer with 89% conversion and 1.4 dispersity under UV light and with 70% conversion and 1.5 dispersity under visible one. A first order kinetic was observed in both cases, confirming an almost constant concentration of radicals, typical of ATRP mechanisms. "On-off" experiments and blank tests confirmed the necessity of all the reagents (light, CDs, initiator and catalyst) in order to obtain the polymer. In comparison with the only other example in the literature, the present procedure was more effective in terms of polymer conversion (70–89% in 1 h versus 30% in 2.5 h) and it allowed to perform ATRP avoiding hazardous solvents (dimethyl sulfoxide was previously used) [16]. In conclusion, a new, cheap and effective photosensitizer for ATR polymerization has been herein studied demonstrating the possibility to achieve greener and efficient processes in polymer preparation.

Fundings

This work was supported by: Nuova Ompi – Stevanato for funding AM's research, Fondazione Cariverona for the project "Valorizzazione di scarti agroalimentari per nuovi cosmetici green" ID n° 1174 – Cod. SIME n° 2019.0428 and Fondazione Cariplo for the project "Photo- and Mechano-Chemistry for the Upgrading of Agro- and Sea-food Waste to advanced polymers and nanocarbon materials", CUBWAM, n° 2021-0751.

CRediT authorship contribution statement

Carlotta Campalani: experimental work, manuscript drafting, Nicola Bragato: experimental work, Andrea Morandini: conceptualization, planning of research, experimental work, Maurizio Selva: conceptualization, management, funding acquisition, Giulia Fiorani: conceptualization, planning, draft manuscript correction, Alvise Perosa: conceptualization, planning, final manuscript correction, management, funding acquisition.

Declaration of Competing Interest

The authors declare the following financial interests/personal relationships which may be considered as potential competing interests: Andrea Morandini reports financial support was provided by Nuova Ompi. Maurizio Selva reports financial support was provided by Cariplo Foundation. Alvise Perosa reports financial support was provided by Fondazione Cariverona.

Data Availability

Data will be made available on request.

Acknowledgments

Giorgia Minello is kindly acknowledged for her help during the experimental part of this project. Nuova Ompi – Stevanato is gratefully acknowledged for supporting AM's research. Fondazione Cariverona is gratefully acknowledged for funding the project "Valorizzazione di scarti agroalimentari per nuovi cosmetici green" ID n° 1174 – Cod. SIME n° 2019.0428. We gratefully acknowledge the support from Fondazione Cariplo (Photo- and Mechano-Chemistry for the Upgrading of Agro- and Sea-food Waste to advanced polymers and nanocarbon materials, CUBWAM, project 2021–0751).

Appendix A. Supporting information

Supplementary data associated with this article can be found in the online version at doi:10.1016/j.cattod.2023.114039.

References

[1] J.-S. Wang, K. Matyjaszewski, Controlled "Living " radical polymerization. atom transfer radical polymerization in the presence of transition-metal complexes, J. Am. Chem. Soc. 117 (1995) 5614–5615, https://doi.org/10.1021/ja00125a035.
[2] M. Kato, M. Kamigaito, M. Sawamoto, T. Higashimura, Polymerization of methyl methacrylate with the carbon Tetrachloride/Dichlorotris(triphenylphosphine) ruthenium(II)/ methylaluminum Bis(2,6-di-tert-butylphenoxide) initiating system: possibility of living radical polymerization, Macromolecules 28 (1995) 1721–1723, https://doi.org/10.1021/ma00109a056.
[3] V. Percec, B. Barboiu, "Living" radical polymerization of styrene initiated by arenesulfonyl chlorides and CuI(bpy)nCl, Macromolecules 28 (1995) 7970–7972, https://doi.org/10.1021/ma00127a057.
[4] S. Dadashi-Silab, M.A. Tasdelen, Y. Yagci, Photoinitiated atom transfer radical polymerization: current status and future perspectives, Polym. Chem. 52 (2014) 2878–2888, https://doi.org/10.1002/pola.27327.
[5] F. Di Lena, K. Matyjaszewski, Transition metal catalysts for controlled radical polymerization, Prog. Polym. Sci. 35 (2010) 959–1021, https://doi.org/10.1016/j.progpolymsci.2010.05.001.

[6] K. Matyjaszewski, W. Jakubowski, K. Min, W. Tang, J. Huang, W.A. Braunecker, N. V. Tsarevsky, Diminishing catalyst concentration in atom transfer radical polymerization with reducing agents, Proc. Natl. Acad. Sci. USA 103 (2006) 15309–15314, https://doi.org/10.1073/pnas.0602675103.
[7] A.J.D. Magenau, N.C. Strandwitz, A. Gennaro, K. Matyjaszewski, Electrochemically mediated atom transfer radical polymerization, Science 332 (2011) (1979) 81–84, https://doi.org/10.1017/cbo9781139167291.033.
[8] K. Matyjaszewski, N.V. Tsarevsky, W.A. Braunecker, H. Dong, J. Huang, W. Jakubowski, Y. Kwak, R. Nicolay, W. Tang, J.A. Yoon, Role of Cu 0 in controlled/"living" radical polymerization, Macromolecules 40 (2007) 7795–7806, https://doi.org/10.1021/ma0717800.
[9] D. Konkolewicz, K. Schröder, J. Buback, S. Bernhard, K. Matyjaszewski, Visible light and sunlight photoinduced ATRP with ppm of Cu catalyst, ACS Macro Lett. 1 (2012) 1219–1223, https://doi.org/10.1021/mz300457e.
[10] M.A. Tasdelen, M. Uygun, Y. Yagci, Photoinduced controlled radical polymerization, Macromol. Rapid Commun. 32 (2011) 58–62, https://doi.org/10.1002/marc.201000351.
[11] M.A. Tasdelen, M. Uygun, Y. Yagci, Photoinduced controlled radical polymerization in methanol, Macromol. Chem. Phys. 211 (2010) 2271–2275, https://doi.org/10.1002/macp.201000445.
[12] M.A. Tasdelen, M. Uygun, Y. Yagci, Studies on photoinduced ATRP in the presence of photoinitiator, Macromol. Chem. Phys. 212 (2011) 2036–2042, https://doi.org/10.1002/macp.201100267.
[13] T.G. Ribelli, D. Konkolewicz, S. Bernhard, K. Matyjaszewski, How are radicals (re) generated in photochemical ATRP, J. Am. Chem. Soc. 136 (2014) 13303–13312, https://doi.org/10.1021/ja506379s.
[14] E.H. Discekici, A. Anastasaki, J. Read De Alaniz, C.J. Hawker, Evolution and future directions of metal-free atom transfer radical polymerization, Macromolecules 51 (2018) 7421–7434, https://doi.org/10.1021/acs.macromol.8b01401.
[15] Y. Yagci, S. Jockusch, N.J. Turro, Photoinitiated polymerization: advances, challenges, and opportunities, Macromolecules 43 (2010) 6245–6260, https://doi.org/10.1021/ma1007545.
[16] C. Kütahya, P. Wang, S. Li, S. Liu, J. Li, Z. Chen, B. Strehmel, Carbon dots as a promising green photocatalyst for free radical and ATRP-Based radical, Angew. Chem. - Int. Ed. 59 (2020) 3166–3171, https://doi.org/10.1002/anie.201912343.
[17] X. Pan, N. Malhotra, A. Simakova, Z. Wang, D. Konkolewicz, K. Matyjaszewski, Photoinduced atom transfer radical polymerization with ppm-Level Cu catalyst by visible light in aqueous media, J. Am. Chem. Soc. 137 (2015) 15430–15433, https://doi.org/10.1021/jacs.5b11599.
[18] C. Kütahya, C. Schmitz, V. Strehmel, Y. Yagci, B. Strehmel, Near-Infrared sensitized photoinduced atom-transfer radical polymerization (ATRP) with a Copper(II) catalyst concentration in the ppm range, Angew. Chem. - Int. Ed. 57 (2018) 7898–7902, https://doi.org/10.1002/anie.201802964.
[19] J. Jiang, G. Ye, Z. Wang, Y. Lu, J. Chen, K. Matyjaszenski, Heteroatom-Doped carbon dots CDs as a class of metal-free photocatalysts for PET-RAFT, Angew. Chem. 130 (2018) 12213–12218, https://doi.org/10.1002/anie.201807385.
[20] J. Du, N. Xu, J. Fan, W. Sun, X. Peng, Carbon dots for in vivo bioimaging and theranostics, Small 15 (2019) 1–16, https://doi.org/10.1002/smll.201805087.
[21] S. Cailotto, E. Amadio, M. Facchin, M. Selva, E. Pontoglio, F. Rizzolio, P. Riello, G. Toffoli, A. Benedetti, A. Perosa, Carbon-dots from sugars and ascorbic acid: role of the precursors on morphology, properties, toxicity and drug uptake, ACS Med. Chem. Lett. 9 (2018) 832–837, https://doi.org/10.1021/acsmedchemlett.8b00240.
[22] H. Choi, S.J. Ko, Y. Choi, P. Joo, T. Kim, B.R. Lee, J.W. Jung, H.J. Choi, M. Cha, J. R. Jeong, I.W. Hwang, M.H. Song, B.S. Kim, J.Y. Kim, Versatile surface plasmon resonance of carbon-dot-supported silver nanoparticles in polymer optoelectronic devices, Nat. Photonics 7 (2013) 732–738, https://doi.org/10.1038/nphoton.2013.181.
[23] G.A.M. Hutton, B.C.M. Martindale, E. Reisner, Carbon dots as photosensitisers for solar-driven catalysis, Chem. Soc. Rev. 46 (2017) 6111–6123, https://doi.org/10.1039/C7CS00235A.
[24] A. Emanuele, S. Cailotto, C. Campalani, L. Branzi, C. Raviola, D. Ravelli, E. Cattaruzza, E. Trave, A. Benedetti, M. Selva, A. Perosa, Precursor-dependent photocatalytic activity of carbon dots, Molecules 25 (2019) 1–9, https://doi.org/10.3390/molecules25010101.
[25] S. Cailotto, M. Negrato, S. Daniele, R. Luque, M. Selva, E. Amadio, A. Perosa, Carbon dots as photocatalysts for organic synthesis: Metal-free methylene-oxygen-bond photocleavage, Green. Chem. 22 (2020) 1145–1149, https://doi.org/10.1039/c9gc03811f.
[26] Y. Xie, S. Yu, Y. Zhong, Q. Zhang, Y. Zhou, SnO 2 /graphene quantum dots composited photocatalyst for efficient nitric oxide oxidation under visible light, Appl. Surf. Sci. 448 (2018) 655–661, https://doi.org/10.1016/j.apsusc.2018.04.145.
[27] C. Campalani, E. Cattaruzza, S. Zorzi, A. Vomiero, S. You, L. Matthews, M. Capron, C. Mondelli, M. Selva, A. Perosa, Biobased carbon dots: from fish scales to photocatalysis, Nanomaterials 11 (2021) 524, https://doi.org/10.3390/nano11020524.
[28] M. Yan, F. Zhu, W. Gu, L. Sun, W. Shi, Y. Hua, Construction of nitrogen-doped graphene quantum dots-BiVO4/g-C3N4 Z -scheme photocatalyst and enhanced photocatalytic degradation of antibiotics under visible light, RSC Adv. 6 (2016) 61162–61174, https://doi.org/10.1039/c6ra07589d.
[29] C. Campalani, G. Petit, M. Selva, A. Perosa, Continuous flow photooxidative degradation of azo dyes with biomass-derived carbon dots, ChemPhotoChem (2022), https://doi.org/10.1002/cptc.202200234.
[30] C. Campalani, V. Causin, M. Selva, A. Perosa, Fish-waste-derived gelatin and carbon dots for biobased UV- blocking films, ACS Appl. Mater. Interfaces 14 (2022) 35148–35156, https://doi.org/10.1021/acsami.2c11749.
[31] S. Cailotto, D. Massari, M. Gigli, C. Campalani, M. Bonini, S. You, A. Vomiero, M. Selva, A. Perosa, C. Crestini, N-Doped carbon dot hydrogels from brewing waste for photocatalytic wastewater treatment, ACS Omega 7 (2022) 4052–4061, https://doi.org/10.1021/acsomega.1c05403.
[32] Q. Hao, L. Qiao, G. Shi, Y. He, Z. Cui, P. Fu, M. Liu, X. Qiao, X. Pang, Effect of nitrogen type on carbon dot photocatalysts for visible-light-induced atom transfer radical polymerization, Polym. Chem. 12 (2021) 3060–3066, https://doi.org/10.1039/d1py00148e.
[33] Z. Zhang, G. Yi, P. Li, X. Zhang, H. Fan, Y. Zhang, X. Wang, C. Zhang, A minireview on doped carbon dots for photocatalytic and electrocatalytic applications, Nanoscale 12 (2020) 13899–13906, https://doi.org/10.1039/d0nr03163a.
[34] K.G. Nguyen, I.A. Baragau, R. Gromicova, A. Nicolaev, S.A.J. Thomson, A. Rennie, N.P. Power, M.T. Sajjad, S. Kellici, Investigating the effect of N-doping on carbon quantum dots structure, optical properties and metal ion screening, Sci. Rep. 12 (2022) 1–12, https://doi.org/10.1038/s41598-022-16893-x.
[35] S. Cailotto, R. Mazzaro, F. Enrichi, A. Vomiero, E. Cattaruzza, D. Cristofori, E. Amadio, A. Perosa, Design of carbon dots for metal-free photoredox catalysis, ACS Appl. Mater. Interfaces 10 (2018) 40560–40567, https://doi.org/10.1021/acsami.8b14188.
[36] N. Soin, S. Sinha Roy, S. Roy, K.S. Hazra, D.S. Misra, T.H. Lim, C.J. Hetherington, J. A. McLaughlin, Enhanced and stable field emission from in situ nitrogen-doped few-layered graphene nanoflakes, J. Phys. Chem. C. 115 (2011) 5366–5372, https://doi.org/10.1021/jp110476m.
[37] K. Matyjaszewski, B. Göbelt, H.J. Paik, C.P. Horwitz, Tridentate nitrogen-based ligands in Cu-based ATRP: a structure-activity study, Macromolecules 34 (2001) 430–440, https://doi.org/10.1021/ma001181s.
[38] M.H. Stenzel, C. Barner-Kowollik, The living dead – common misconceptions about reversible deactivation radical polymerization, Mater. Horiz. 3 (2016) 471–477, https://doi.org/10.1039/c6mh00265j.
[39] W. Tanan, J. Panichpakdee, S. Saengsuwan, Novel biodegradable hydrogel based on natural polymers: Synthesis, characterization, swelling/reswelling and biodegradability, Eur. Polym. J. 112 (2019) 678–687, https://doi.org/10.1016/j.eurpolymj.2018.10.033.
[40] K. Roa, Y. Tapiero, M.O. Thotiyl, J. Sánchez, Hydrogels based on poly([2-(acryloxy)ethyl] trimethylammonium chloride) and nanocellulose applied to remove methyl orange dye from water, Polymer 13 (2021), https://doi.org/10.3390/polym13142265.
[41] J. Sánchez, N. Mendoza, B.L. Rivas, L. Basáez, J.L. Santiago-García, Preparation and characterization of water-soluble polymers and their utilization in chromium sorption, J. Appl. Polym. Sci. 134 (2017) 1–10, https://doi.org/10.1002/app.45355.
[42] M.A. Cismesia, T.P. Yoon, Characterizing chain processes in visible light photoredox catalysis, Chem. Sci. 6 (2015) 5426–5434, https://doi.org/10.1039/c5sc02185e.